

Experimental Assessment of Misalignment Effects in Terahertz Communications

Hasan Nayir*, Erhan Karakoca*[†], Güneş Karabulut Kurt[‡], Ali Görçin*[†]

* Department of Electronics and Communication Engineering, İstanbul Technical University, İstanbul, Turkey

[†] Communications and Signal Processing Research (HİSAR) Laboratory, TÜBİTAK BİLGEM, Kocaeli, Turkey

[‡] Poly-Grames Research Center, Department of Electrical Engineering, Polytechnique Montréal, Montréal, QC, Canada

Emails: {nayir20, karakoca19}@itu.edu.tr, gunes.kurt@polymtl.ca, ali.gorcin@tubitak.gov.tr

Abstract—Terahertz (THz) frequencies play a crucial role in the advancement of next-generation wireless systems, primarily owing to their substantial available bandwidths. The inherent limitation of limited range, attributed to high attenuation in these frequencies, can be effectively addressed by implementing densely deployed heterogeneous networks, complemented by Unmanned Aerial Vehicles (UAVs) within a three-dimensional hyperspace. Yet, the success of THz communications relies on the precise alignment of beams. Inadequate handling of beam alignment can lead to diminished signal strength at the receiver, significantly affecting THz signals more than their conventional counterparts. This research underscores the paramount importance of meticulous alignment in THz communication systems. The profound impact of proper alignment is substantiated through comprehensive measurements conducted using a state-of-the-art measurement setup, facilitating accurate data collection across the 240 GHz to 300 GHz spectrum. These measurements encompass varying angles and distances within an anechoic chamber to eliminate reflections. Through a meticulous analysis of the channel frequency and impulse responses derived from these extensive measurements, this study pioneers quantifiable results, providing an assessment of the effects of beam misalignment in THz frequencies.

Index Terms—Terahertz communications, unmanned aerial vehicles (UAVs), channel frequency response, channel impulse response.

I. INTRODUCTION

While the need for high data rates is still on the agenda, the 6G vision has highlighted various key value indicators (KVI) such as global coverage, service availability, sustainability, and reliability. When we set out with the “connection in anywhere, anytime, any device” motto, there is no doubt that aerial systems will be the most prominent candidate to bring access to urban, semi-urban, and remote rural areas. Adding aerial base stations for improving the quality of service (QoS) and boosting the coverage, reliability and capacity of wireless networks has been suggested in the academy for a while [1]–[3]. In addition to bringing fast deployment features to non-terrestrial networks (NTNs), unmanned aerial vehicles (UAVs) also acts as a bridge between terrestrial networks (TNs) and other non-terrestrial network elements such as satellites and high altitude platforms (HAPs).

Terahertz (THz) wireless systems are expected to be a vital enabler for 6G in tandem with TNs and NTNs because of

their large contiguous bandwidth [4] which allows them to keep pace with the surge in wireless data volume and the increasing amount of traffic as new nodes are added to the network. Likewise, considering the fact that THz bands are not allocated yet for specific active services around the globe, there is an enormous potential to meet the need for the desired communication traffic. Hence the orchestration of NTN and TNs with the THz communication is apparent towards 6G [5].

Along with their benefits, THz frequencies also come with high attenuation due to molecular absorption and spreading loss [6], which limits the communication range significantly. Addressing these limitations demands innovative THz communication systems. This is where UAVs come into play as a remedy especially to provide instant high-capacity communication links in crowded environments or to support high-capacity data traffic between different TN and NTN nodes [7]. Moreover, along with their cost-effectiveness and instant 3D deployment capabilities which allow maintaining line-of-sight (LoS) condition for the communication links, UAVs also provides flexibility to the network nodes. UAVs and THz are strong collaborators by their nature and this mutually constructive relationship, in turn, can unlock new opportunities and innovative services [8]. Thus, UAVs are expected to pave radically the way for assisting THz communications.

While THz-integrated UAVs presents promising prospects they also bring new challenges to the field. Although the utilization of directional beamforming unified with directional antennas can provide higher antenna gains to reduce the high transmission loss in the THz frequency range, these systems are prone to pointing errors due to small beamwidths. Moreover, wind or sudden complex movements can cause uncontrollable tilts or rotations in UAV operations, leading to beam misalignment and an inevitable decrease in signal-to-noise ratio (SNR). Accordingly, UAV-assisted THz communication requires accurate beam alignment mechanisms and algorithms. As we move towards the development of 6G networks and the realization of THz communication systems, it is crucial to conduct a comprehensive investigation of misalignment scenarios. This involves analyzing and modeling the potential effects of the misalignment on specific applications.

A. Related Works

The antenna misalignment effects on THz communication systems have been investigated across various environments and frequency ranges, but mostly by simulations [9]–[12]. In particular, [9] and [10] examined the effects of antenna misalignment at 300 GHz in a simulated office setup by considering practical propagation conditions. In [11], the performance of a multicarrier THz wireless system is evaluated under the fading condition caused by misalignment. The effects of pointing error impairments under random fog conditions are examined in [12].

On the other hand, measurement based impact of misalignment has been analysed in [13], [14]. The authors in [13] carried out measurements to analyze the impact of the distance and single degree of misalignment on the path loss in the THz communication system and several important statistical parameters for line-of-sight (LOS) channels are measured. The performance of the experimental THz communication systems has been examined in case of antenna misalignment at 100, 300, 400 and 500 GHz by utilizing proper horn antennas in the [14]. A significant decrease trend was indicated in the received power with misalignment due to the divergence of the beams particularly with an increase in separation distance. Also, the new modelling technique for measurement-based THz channels is proposed in [15] and regarding this model capacity analysis is given in [16]. Most importantly, the authors in [17] have designed a drone-based measurement setup to investigate the effects of mobility uncertainties on mmWave/THz-band communications between flying drones. The authors showed that the mobility of the UAVs when they are in movement causes significant performance degradation and link outages while propeller rotation and engine operations of the UAVs cause far less performance degradation.

B. Contributions

In order to fully maximize the potential of THz communication systems, a deep understanding of their performance in practical conditions is required. As the realization of the UAV-assisted THz communication becomes increasingly prevalent, the effect of misalignment becomes a more prominent concern. Addressing this issue necessitates a more comprehensive approach, as prior studies have only partially explored the impact of distance and antenna misalignment on THz communication. To achieve this, it is essential to gather application-specific measurements and conduct an in-depth analysis of their impact on channel frequency and impulse response. In the light of these motivations, our contributions are listed as follows:

- Undertaking precise controlled THz misalignment experiments is a formidable task that requires extensive expertise and experience. To unravel the intricacies involved, a groundbreaking measurement system has been devised to capture precise measurements under varying misalignment scenarios and at different distances. Moreover, this study strives to illuminate future research endeavours by providing a comprehensive explication of the measure-

ment campaign and sharing invaluable insights derived from a multidisciplinary approach.

- Also, recognizing the significance of large bandwidths in practical THz communication systems, this study stands apart from the majority of existing literature on THz measurements. Rather than focusing solely on a specific frequency range, measurements were conducted using a single scan method, encompassing the 60 GHz band and spanning from 240 GHz to 300 GHz.
- The measurements were analyzed in terms of the channel frequency and impulse responses to gain insights into the joint effect of the distance and misalignment.

C. Organization

The remainder of this paper is organized as follows: in Section II, the signal model is introduced, providing a foundational understanding of the system. Subsequently, the measurement campaign is explained, outlining the approach and methodology employed. The obtained measurement results are presented in Section III, showcasing valuable findings and insights. Finally, the conclusion and future directions are discussed in Section IV, summarizing the key outcomes and presenting potential avenues for further research.

II. SIGNAL MODEL AND SYSTEM OVERVIEW

In this study, the effect of misalignment for THz channels is investigated in the anechoic chamber. The traditional linear, time-invariant channel model approach is used to reduce complexity in the analysis.

A. Signal Model

The received signal at the passband can be expressed as

$$r(t) = \text{Re} \{ (x_I(t) + jx_Q(t)) e^{j2\pi f_c t} \}, \quad (1)$$

where f_c denotes the carrier frequency. Also, $x_I(t)$ and $x_Q(t)$ are the in-phase and quadrature components of the received signal, respectively. The received signal can be modeled as a superposition of multipath signals with different delays and complex gains. So, the channel at the baseband can be represented as

$$h(t) = \sum_{l=0}^{L-1} \alpha_l e^{-j2\pi f_c t_l} \delta(t - t_l), \quad (2)$$

where L , α_l , and t_l represent the number of multipath components, channel complex gain, and delay for the l -th path, respectively. As we have mentioned before, measurements have been carried out in a fully isolated anechoic chamber, so we can assume there is only LoS signal transmission. Thus, LoS channels can be derived for $L = 1$ (2) as

$$h(t) = a_f e^{j\theta} \delta(t - t_0), \quad (3)$$

where a_f , θ , and $t_0 = d/c$ denote the LoS path complex gain, phase of the signal, and propagation delay, respectively. Also, d is the distance between the transmitter and receiver, and c is the speed of the light. It is crucial to acknowledge that when using directional antennas, which is a common practice

in THz communication, the effects of antenna misalignment, frequency-dependent loss, and frequency dispersion index can all be accounted for by the term a_f .

In existing literature, the stochastic characterization of multipath components in a static environment is commonly regarded as a combination of specular and diffused components, forming a superposition [18].

$$\begin{aligned} m_l &= a_l e^{-i2\pi f c t} \\ &= s_l + d_l \end{aligned} \quad (4a)$$

$$s_l = \sigma_{s_l} e^{(j2\pi f_0 \cos(\theta_l) + \phi_l)} \quad (4b)$$

$$d_l = \sigma_{d_l} \frac{1}{\sqrt{M_l}} \sum_{m=1}^{M_l} b_m e^{(j2\pi f c \cos(\theta_m) + \phi_m)} \quad (4c)$$

where the term σ_{s_l} represents the magnitude of the specular component, while θ_l denotes the angle of arrival (AoA) and ϕ_l represents the phase of the specular component. Similarly, σ_{d_l} corresponds to the magnitude of the diffused component, M_l signifies the number of diffused waves, b_m represents the amplitude of the incoming waves, θ_m denotes the AoA, and ϕ_m is the phase of the incoming waves forming the diffused component, respectively. It is commonly assumed, without loss of generality, that both σ_{s_l} and σ_{d_l} can be considered as unity under ideal conditions.

The LoS scenario stands out as a special case in wireless propagation, exhibiting inherent characteristics in both large-scale and small-scale fading mechanisms. To guarantee LoS transmission, it is crucial to implement a fully isolated measurement setup within an anechoic chamber, incorporating absorbers. This setup effectively limits the losses introduced by the propagation channel to factors such as distance-dependent path loss, potential antenna misalignments, equipment imperfections, and non-ideal behaviors that may arise when operating in proximity to or above ideal conditions.

In this model, the losses are contingent upon both the distance and misalignment between the transmitter and receiver. When taking into account the distance and angular losses associated with a directional antenna having a maximum gain direction angle φ , the loss can be expressed in decibels dB as follows:

$$PL = PL_0 + 10n \log_{10}(d) + \mathbb{G}(\phi - \varphi), \quad (5)$$

d is the distance between the extender modules. \mathbb{G} represents the normalized angular gain pattern of an antenna and ϕ is the angle between the extender modules.

The angular gain function in linear scale can be approximated as [19]

$$G(\theta) = \left| \frac{\sin(\omega\theta)}{\omega\theta} \right|, \quad |\theta| \leq \pi, \quad (6)$$

where ω is a parameter linked to both the maximum gain direction angle and the beamwidth of the directional antenna. The antenna beamwidth can be defined as twice the angular value at which the measured power in the maximum gain direction decreases by half.

B. Measurement Setup

One of the most critical factors to be considered in misalignment experiments is ensuring the repeatability of certain scenarios and settings of the measurements. Especially when the focus is on THz frequencies various factors must be considered where even the slightest change can significantly impact the results. Foremost, maintaining the accuracy of the 0° position, serving as the reference for misalignment assessment, is crucial. Periodic verification of the alignment at other angles is equally important. Thus, a rotation platform has been engineered to facilitate precise adjustments of horizontal angles, offering seamless transitions at one-degree intervals. To maintain a consistent distance during receiver rotation, it is crucial to place the antenna precisely at the center of the rotation platform. To guarantee the consistency of measurements, the mobile rotation platform should be configured in a manner that allows for periodic recalibration without the need to disassemble the extenders. Such a process that starts from designing the measurement setup that serves a particular purpose and reaches the results verified by repeated measurements obliges carrying out a multi-disciplinary effort. Misalignment is controlled by the angular rotation of the receiver. The mini slide rail facilitates calibration by bringing the extenders closer without necessitating their removal from the setup, with the indexing plunger effectively preventing undesired angle changes. This measurement setup not only enables the assessment of misalignment but also allows for distance-dependent measurements, given the mobility of the rotation platforms with rails. Also, effective cable management is essential to maintain signal integrity and minimize interference. It's essential to use high-quality cables with proper shielding, particularly when operating at high frequencies, to mitigate signal losses and ensure reliable transmission. For this study, Minicircuit branded cables are preferred for their low-loss characteristics. Likewise, regular calibration of measurement equipment, including antennas and extenders, is paramount to maintain precision and compensate for any variations or fluctuations in performance. This involves comparing measured signals with established reference standards. Moreover, meticulous control over the experimental environment is vital to minimize the influence of external factors like temperature, humidity, and electromagnetic interference on the measurements. By adhering to these design guidelines, a robust measurement setup can be created that actively minimizes the impact of external factors, resulting in reproducible accurate and reliable measurements.

1) *Description of Measurement Setup:* Our THz experimental setup is shown in Fig. 2 which is constructed in the MİLTAL at the TÜBİTAK. The measurement setup consists of four main hardware parts and mechanical parts. Hardware parts of the system consist of Agilent vector network analyzer (VNA) E8361A, Oleson Microwave Labs (OML) V03VNA2-T and V03VNA2-T/R-A millimetre wave extender modules and N5260A extender controller.

To enable the analysis of misalignment effects on the THz

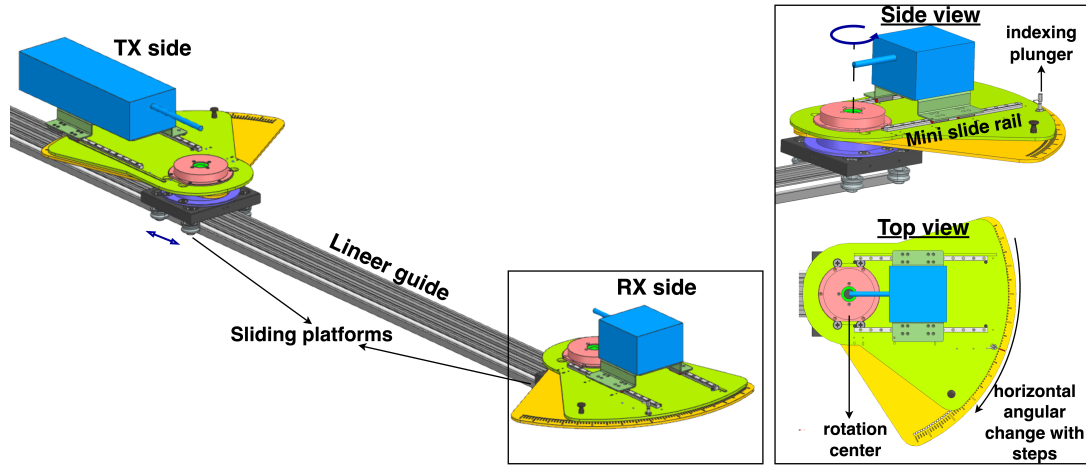


Fig. 1. A three-dimensional (3D) model depicting the mechanical components of the measurement setup, including a rotating mechanism with 1-degree precision in the horizontal direction and an adjustable horizontal distance between the transmitter and receiver.

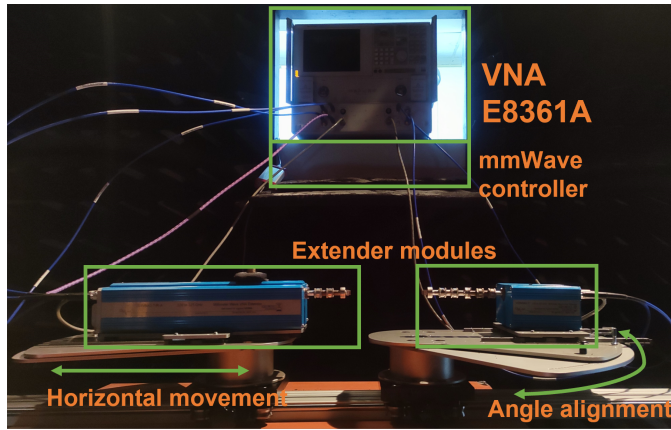


Fig. 2. Measurement setup.

TABLE I
MEASUREMENT PARAMETERS

| Description | Value |
|------------------------------|----------------------------------|
| Operating frequency | 240GHz - 300GHz |
| Bandwidth | 60GHz |
| Measurement frequency points | 4096 |
| IF bandwidth | 100Hz |
| Spectral resolution | 14.648MHz |
| Antenna misalignment | 0° : 1° : 15° and 15° : 5° : 30° |
| Distance (cm) | 20:10:100cm |

which is limited to an operational frequency of 67 GHz. The V03VNA2-T/R-A drives up the RF signal within the 12.2 GHz and 18.1 GHz range by a factor of 18 and expands the frequency of the transmission signals allowing VNA to analyze signals between 220 GHz and 325 GHz. Before transmission, the VNA acquires test intermediate frequency (IF) and reference IF signals through downconversion mixers. Following signal reception after passing through the channel, it undergoes downconversion at V03VNA2-T which results in a test IF signal that is fed back to the VNA for further analysis. The extender modules have been driven by an extended band WR-10 multiplier chain with a waveguide output interface. The waveguide output power of the V03VNA2-T/R-A is around -23 dBm. Also, the magnitude and phase stability of the extenders are $\pm 0.4\text{dB}$ and $\pm 8^\circ$, respectively. Also, a half-power beam width horn antenna with 25 dBi gain [20] is used in measurements. Because of the narrow beamwidth at high frequencies, the alignment between the transmitter and receiver needs to be very precise. So, the extender modules have been installed in a mechanical system as mentioned in Section II-B where we can precisely change the distance and angles between the modules.

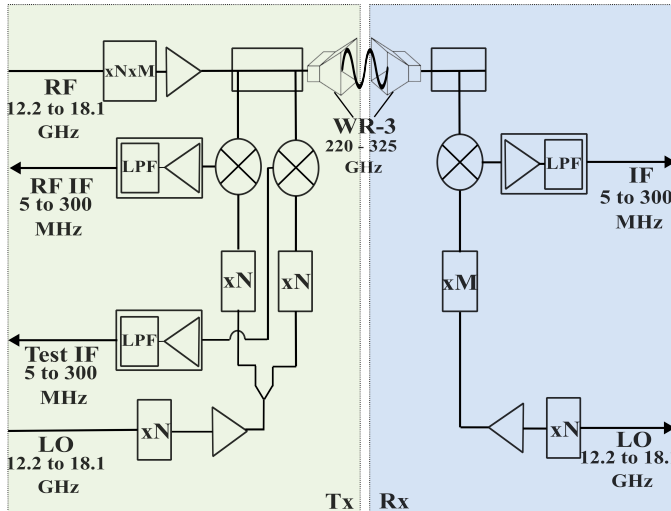


Fig. 3. Block diagram of transmitter and receiver extenders.

frequency range, extender modules are coupled with the VNA

2) *Measurement Methodology*: In this study, the operating frequency range is set to 240 GHz to 300 GHz because of the magnitude and phase stability of the extender modules in this range. To ensure accuracy, the spectral resolution of each

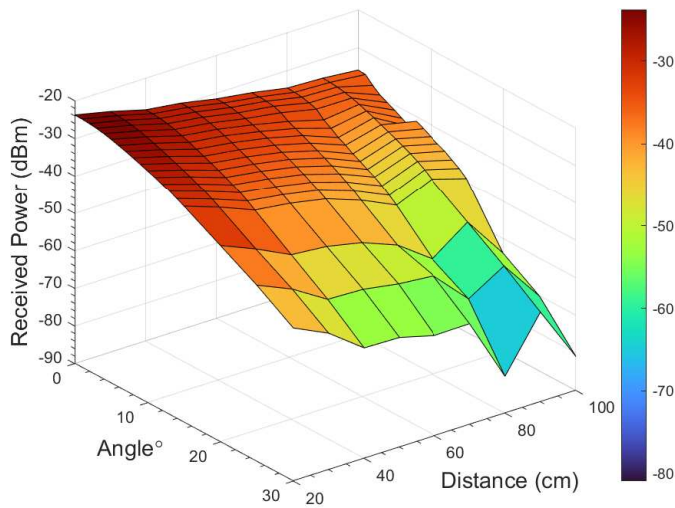


Fig. 4. Maximum values of the channel impulse response for all distances and antenna misalignment degrees.

TABLE II
RECEIVED SIGNAL PEAK POWERS AT ALL DISTANCES AND ANTENNA MISALIGNMENTS

| | 0° | 5° | 10° | 15° | 20° | 25° | 30° |
|--------|--------|--------|--------|--------|--------|--------|--------|
| 20 cm | -23.77 | -25.02 | -28.19 | -32.48 | -37.79 | -43.13 | -49.29 |
| 30 cm | -25.86 | -27.35 | -30.95 | -35.78 | -41.71 | -47.17 | -53.70 |
| 40 cm | -28.42 | -30.07 | -34.02 | -39.52 | -46.24 | -52.90 | -56.92 |
| 50 cm | -29.66 | -31.38 | -35.40 | -40.74 | -47.07 | -53.25 | -60.85 |
| 60 cm | -31.55 | -33.21 | -37.16 | -42.56 | -49.05 | -54.82 | -62.07 |
| 70 cm | -32.92 | -35.32 | -39.82 | -45.93 | -52.73 | -55.68 | -63.20 |
| 80 cm | -34.71 | -37.92 | -42.03 | -46.13 | -50.92 | -56.15 | -60.51 |
| 90 cm | -35.11 | -36.84 | -40.76 | -46.27 | -52.59 | -59.08 | -66.16 |
| 100 cm | -35.98 | -39.92 | -43.17 | -49.14 | -52.67 | -57.57 | -63.02 |

measurement is set to be 14.648 MHz, which corresponds to 4096 frequency points with an IF bandwidth of 100 Hz. To ensure accurate measurements, it is necessary to calibrate electronic devices and cables together. Prior to the measurements, calibration was done by connecting the waveguide ports of the transmitter and receiver modules end-to-end to retrieve any unwanted effects caused by the electronics. So as to comprehensively investigate the impact of antenna misalignment on received power in the THz wireless channel, a series of measurements were conducted using a sliding rail and rotation platform. These platforms enabled horizontal angle adjustments with a precision of 1° at each distance setting, allowing for a comprehensive investigation of the influence of antenna misalignment with distance.

In order to facilitate analysis and improve the reliability of data by minimizing the number of unknown variables, this study specifically evaluated changes in only the horizontal angle. By narrowing the scope to changes in the horizontal angle, the research yielded more precise and trustworthy findings. The measurements were obtained as S_{21} parameters and stored as complex numbers in Agilent VNA E8361A. The parameters of the measurements are presented in detail in Table I.

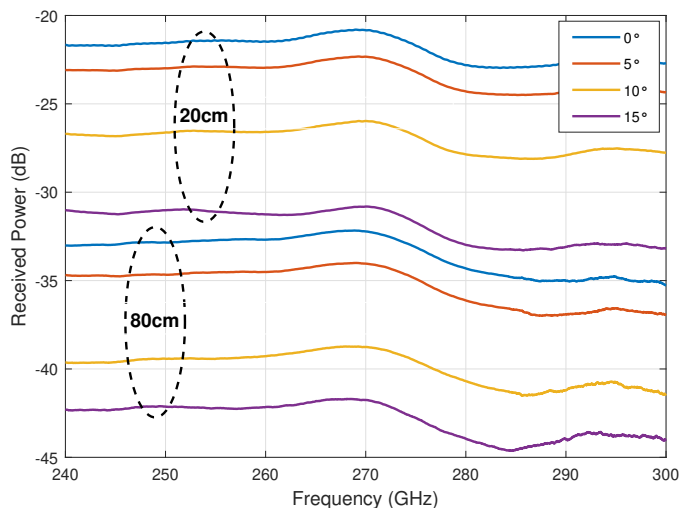


Fig. 5. Channel frequency responses with 0°, 5°, 10° and 15° antenna misalignment at 20cm and 80cm distances.

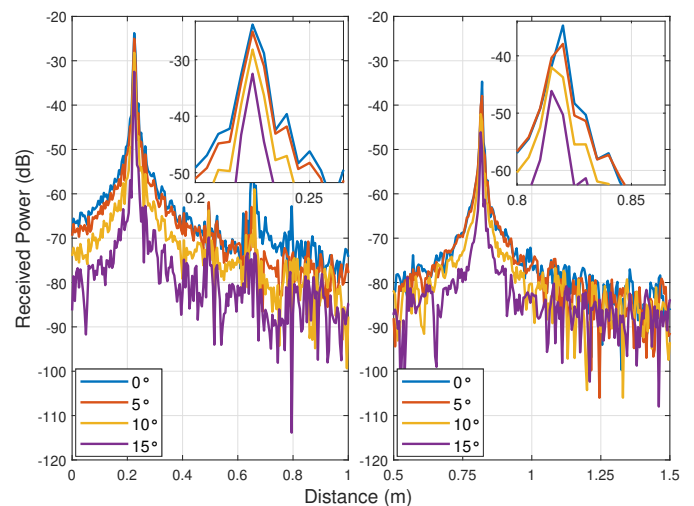


Fig. 6. Channel impulse responses with 0°, 5°, 10° and 15° antenna misalignment at 20 cm and 80 cm distances.

III. MEASUREMENT RESULTS

In this section, the joint impact of the antenna misalignment and the distance dependent path loss is presented by illustrating the channel frequency response and impulse response of the measurements. The channel frequency responses for 0, 5, 10 and 15-degree antenna misalignment at 20 cm and 80 cm are shown in Fig. 5. If only the distance between the transmitter and receiver is taken into account, the received power experiences a change of approximately 12 dB when the separation is increased from 20 cm to 80 cm. The 15-degree horizontal angle change from the reference point at 20 cm causes the 8 dB reduction of the received power.

For example, the received power difference is around 12 dB without antenna misalignment for 20 cm and 80 cm. In case of antenna misalignment, loss of the received power can reach up to 8 dB. In addition, Fig. 6 shows that time domain analysis by taking inverse Fourier Transform of the measurement data. In

this figure, it is seen that there is a decrease in received power due to antenna misalignment. So, antenna misalignment considerably impacts received signal power because THz antennas have a narrow beam width. Furthermore, Fig. 4 illustrates the channel impulse response with the combined distance and antenna misalignment measurements. It is plotted using the max value of the channel impulse response for every distance and angle measurement pair. In addition, the direct numerical value equivalents of these measurement pairs are given in the Table II. Given that increasing the separation between the transmitter and the receiver from 20 cm to 80 cm results in a received power loss nearly equivalent to the loss incurred by a 10-degree antenna misalignment at a distance of 80 cm, the estimated loss in both scenarios is approximately 9 dB.

Antenna misalignment is an indispensable concern for THz communication systems in UAVs, as it directly impacts the received power. The distance between the transmitter and receiver is the primary factor in diminishing received power, with antenna misalignment exacerbating this power loss and causing a further decrease in received power. In this context, the development of fast and robust beamforming and beam tracking algorithms is imperative for UAVs equipped with THz communication systems. Compensating for misalignment is crucial for various reasons, ensuring a consistent level of received power and reliable communication in UAVs operating at THz frequencies.

IV. CONCLUSION AND FUTURE DIRECTIONS

THz communication systems hold promise as a solution for addressing the high data rate demands and increasing number of wireless devices, and UAVs have been featured to enable ubiquitous access to the sublime potential of these frequencies. This study initiates a discussion on antenna misalignment in UAV-assisted THz communication, which will be one of the most critical challenges in the practical implementation step. Experiments were conducted with a fine-tuned setup to explore the impact of horizontal misalignment and distance on received power between 240 GHz and 300 GHz, revealing a significant impact on SNR even minor deviations in alignment. To guide future research, essential factors for misalignment experiments are outlined. The next step involves examining both horizontal and vertical misalignment factors for their joint effects on received power. Furthermore, with advancements in transceiver technology and the feasibility of UAV-mounted THz campaigns, real-world experiments should be conducted.

ACKNOWLEDGMENT

This work has received funding from the AIMS5.0 project. AIMS5.0 has been accepted for funding within the Key Digital Technologies Joint Undertaking (KDT JU), a public-private partnership in collaboration with the HORIZON Framework Programme and the national Authorities under grant agreement number 101112089.

REFERENCES

[1] M. Mozaffari, W. Saad, M. Bennis, and M. Debbah, "Drone small cells in the clouds: Design, deployment and performance analysis," in *2015 IEEE Global Communications Conference (GLOBECOM)*, 2015, pp. 1–6.

[2] M. J. Sobouti, A. H. Mohajzadeh, S. A. H. Seno, and H. Yanikomeroglu, "Managing sets of flying base stations using energy efficient 3D trajectory planning in cellular networks," *IEEE Sensors Journal*, 2023.

[3] M. Giordani, M. Polese, M. Mezzavilla, S. Rangan, and M. Zorzi, "Toward 6G networks: Use cases and technologies," *IEEE Communications Magazine*, vol. 58, no. 3, pp. 55–61, 2020.

[4] A.-A. A. Boulogeorgos, A. Alexiou, T. Merkle, C. Schubert, R. Elschner, A. Katsiotis, P. Stavrianos, D. Kritharidis, P.-K. Chartsias, J. Kokkonniemi *et al.*, "Terahertz technologies to deliver optical network quality of experience in wireless systems beyond 5G," *IEEE Communications Magazine*, vol. 56, no. 6, pp. 144–151, 2018.

[5] K. Tekbiyik, A. R. Ekti, G. K. Kurt, A. Gorcin, and H. Yanikomeroglu, "A holistic investigation of terahertz propagation and channel modeling toward vertical heterogeneous networks," *IEEE Communications Magazine*, vol. 58, no. 11, pp. 14–20, 2020.

[6] J. M. Jornet and I. F. Akyildiz, "Channel modeling and capacity analysis for electromagnetic wireless nanonetworks in the terahertz band," *IEEE Transactions on Wireless Communications*, vol. 10, no. 10, pp. 3211–3221, 2011.

[7] M. M. Azari, S. Solanki, S. Chatzinotas, and M. Bennis, "THz-empowered UAVs in 6G: Opportunities, challenges, and trade-offs," *IEEE Communications Magazine*, vol. 60, no. 5, pp. 24–30, 2022.

[8] M. M. Azari, S. Solanki, S. Chatzinotas, O. Kodheli, H. Sallouha, A. Colpaert, J. F. M. Montoya, S. Pollin, A. Haqiqatnejad, A. Mostaani *et al.*, "Evolution of non-terrestrial networks from 5G to 6G: A survey," *IEEE Communications Surveys & Tutorials*, 2022.

[9] S. Priebe, M. Jacob, and T. Kürner, "The impact of antenna directivities on THz indoor channel characteristics," in *2012 6th European Conference on Antennas and Propagation (EUCAP)*. IEEE, 2012, pp. 478–482.

[10] —, "Affection of THz indoor communication links by antenna misalignment," in *2012 6th European Conference on Antennas and Propagation (EUCAP)*. IEEE, 2012, pp. 483–487.

[11] E. N. Papatotiriou, A.-A. A. Boulogeorgos, and A. Alexiou, "Performance analysis of THz wireless systems in the presence of antenna misalignment and phase noise," *IEEE Communications Letters*, vol. 24, no. 6, pp. 1211–1215, 2020.

[12] O. S. Badarneh, "Performance analysis of terahertz communications in random fog conditions with misalignment," *IEEE Wireless Communications Letters*, vol. 11, no. 5, pp. 962–966, 2022.

[13] A. R. Ekti, A. Boyaci, A. Alparlan, İ. Ünal, S. Yarkan, A. Görçin, H. Arslan, and M. Uysal, "Statistical modeling of propagation channels for terahertz band," in *2017 IEEE Conference on Standards for Communications and Networking (CSCN)*. IEEE, 2017, pp. 275–280.

[14] F. Sheikh, Y. Zantah, M. Al-Hasan, I. Mabrouk, N. Zarifeh, and T. Kaiser, "Horn antenna misalignments at 100, 300, 400, and 500 ghz in close proximity communications," in *2021 IEEE International Symposium on Antennas and Propagation and USNC-URSI Radio Science Meeting (APS/URSI)*. IEEE, 2021, pp. 449–450.

[15] E. Karakoca, G. Karabulut Kurt, and A. Görçin, "Hierarchical Dirichlet process based Gamma mixture modeling for terahertz band wireless communication channels," *IEEE Access*, vol. 10, pp. 84 635–84 647, 2022.

[16] E. Karakoca, H. Nayir, G. K. Kurt, and A. Görçin, "Measurement-based modeling of short range terahertz channels and their capacity analysis," in *GLOBECOM 2023 - 2023 IEEE Global Communications Conference*, 2023, pp. 1471–1476.

[17] Z. Guan and T. Kulkarni, "On the effects of mobility uncertainties on wireless communications between flying drones in the mmwave/thz bands," in *IEEE INFOCOM 2019-IEEE Conference on Computer Communications Workshops (INFOCOM WKSHPS)*. IEEE, 2019, pp. 768–773.

[18] S. Yarkan and H. Arslan, "Identification of los in time-varying, frequency selective radio channels," *EURASIP Journal on wireless communications and networking*, vol. 2008, pp. 1–14, 2008.

[19] H. Zang, F. Baccelli, and J. Bolot, "Bayesian inference for localization in cellular networks," in *2010 Proceedings IEEE INFOCOM*. IEEE, 2010, pp. 1–9.

[20] RFecho, "25 dBi Gain 220GHz-325GHz WR-03 Waveguide Millimeter SGH Antenna," <https://www.rfecho.com/product/25-dbi-gain-220-ghz-to-325-ghz-wr-03-waveguide-millimeter-sgh-antenna>, [Online; accessed: October 19, 2023].